Microstructure formation and abrasive wear resistance of a boron-modified superduplex stainless steel produced by spray forming

Juliano Soyama,[a] Guilherme Zepon, Thiago Pama Lopes, Leamar Beraldo, Claudio Shyinti Kiminami, Walter José Botta, and Claudemiro Bolfarini
Departamento de Engenharia de Materiais (DEMa), Universidade Federal de São Carlos, 13565-905 São Carlos, Brazil

(Received 21 June 2016; accepted 24 August 2016)

The microstructure formation and wear resistance of a superduplex stainless steel modified with the addition of 3 wt% boron produced by spray forming were investigated. Thermodynamic simulations were used as comparison basis and to explain the experimentally observed microstructure, which was composed by primary M_2B-type borides, an austenitic-ferritic matrix, and eutectic M_3B_2-type borides. The predicted solidification sequence started with the precipitation of primary M_2B boride, followed by ferrite/austenite formation and a final eutectic reaction resulting in M_3B_2 borides. A good correlation with the simulations and final microstructure was found. The abrasive wear resistance was investigated with the dry sand/rubber wheel test and the results indicated an outstanding performance, similar to the cobalt-based Stellite 1016 alloy. The excellent wear resistance resulted from the presence of a significant amount (about 35 vol%) of hard borides homogeneously dispersed in the microstructure, which was effective at increasing hardness and protecting the duplex matrix against abrasion.

I. INTRODUCTION

Stainless steels are the material of choice for structural applications that require a good balance of mechanical strength and corrosion resistance.[1,2] For some specific demanding conditions, such as in the offshore industry, there are grades available with exceptional resistance to corrosion, for instance, the superduplex steels.[3] The duplex microstructure is based on balanced phase fractions of ferrite and austenite, whereas the term superduplex is defined based on the pitting resistance equivalent number (PREN: wt%Cr + 3.3 wt%Mo + 16 wt%N) larger than 40.[4] When compared to regular ferritic or austenitic stainless steels, the superduplex series show higher strength, improved local pitting and stress corrosion cracking resistance.[5] Despite the exceptional corrosion resistance of these stainless steel grades, depending on the application conditions, the wear resistance might be rather unsatisfactory.[6] For instance, in components from offshore or chemical process industries where superduplex steels are used due to the corrosion resistance, but are simultaneously subjected to metal to metal moving interfaces (pumps, valves, bearings, etc.). Therefore, methods to improve the wear behavior have been extensively investigated.[7–9] The most common approach is the application of coatings or surface modifications, in which the wear resistance originates from a wear resistant material deposited at the surface.[10–12]

From this point of view, developing coating materials which increase wear resistance of the stainless steel parts while keeping their corrosion properties is an interesting strategy. Recently, Zepon et al.[13] reported the development of the spray-formed boron-modified supermartensitic stainless steel grades with different boron contents. The authors have shown that the addition of boron contents ranging from 0.3 wt% to 0.7 wt% led to the formation of a eutectic network of M_2B-type borides uniformly distributed around the equiaxed grains (typically found in spray-formed alloys). The presence of such hard borides in the microstructure increased significantly the alloys' wear resistance. The accumulated worn volume measured in a plate-on-cylinder wear test was practically 10-fold lower when compared to the conventional supermartensitic stainless steel without boron. Moreover, the authors have demonstrated that if the Cr content of the martensitic matrix stays above 11 wt%, the corrosion resistance of the spray-formed boron-modified alloys no longer differs from the conventional supermartensitic stainless steel.

Furthermore, Sigolo et al.[14] showed that boron-modified supermartensitic and superduplex steel atomised powders could be successfully applied by Plasma Transferred Arc onto low alloy steel substrate. In this case, the amounts of boron addition were 1 wt% and 3 wt% for the supermartensitic and superduplex, respectively.

Contributing Editor: Jürgen Eckert
[a]Address all correspondence to this author.
e-mail: julianosoyama@gmail.com
DOI: 10.1557/jmr.2016.323

The wear resistance of the coatings measured with the pin-on-plate test was far superior in comparison to the substrate material. This improvement was caused by the presence of hard borides (M_2B and M_3B_2-types) in the microstructure. These boride particles also occurred in a representative volume fraction of around 30% for the superduplex composition. Despite the fact that borides might contain Fe, Cr, and Mo, the content of Cr in the matrix could be kept within a reasonable value (>10 wt%).

Spray forming is an advanced deposition process that offers a great advantage of achieving refined microstructures with equiaxed grains in most alloy systems,[13,15–20] in addition to the possibility of near-net-shaping. The process consists basically in a continuous gas atomization of a molten metal stream that is transformed into a spray of droplets. The spray is directed at a substrate to form a billet, which is ultimately subjected to slow cooling.[15] This processing technique is also suitable for large-scale production of homogeneous low defect materials of several different shapes such as sheet, rings, or tubes.[21] Additionally, spray forming has the ability to produce alloy compositions that are problematical in conventional casting processes. For instance, high-alloyed tool steels when manufactured in conventional casting processes present high levels of segregation and inhomogeneous microstructures regarding size and distribution of carbides, which can negatively affect mechanical properties. On the other hand, spray-formed high-alloyed steels such as AISI D2 and AISI M3, present fine and homogeneous microstructure with equiaxed grains.[21] Therefore spray forming seems to be a good candidate for processing these types of materials with significant quantities of alloying elements that might suffer from segregation problems.

Moreover, the microstructure formation of spray forming in the case of tool steels and boron-modified steels have been recently investigated in detail by Zepon et al.[22] The authors reported that the solidification sequence of these materials followed the alloys' equilibrium solidification sequence and that the final microstructure could be easily predicted with the knowledge of the equilibrium phase diagram. In the mentioned work, a solidification model that explain microstructure formation of spray-formed steels was proposed. However, up to now, there is only little experimental work conducted on spray forming of superduplex stainless steels. Consequently, a more in-depth investigation of the microstructure formation is essential for further understanding the solidification sequence and validation of the spray forming solidification model proposed in the literature.

This work presents a first attempt to produce a spray-formed boron-modified superduplex stainless steel, as well as describing its microstructure formation. The starting material was a superduplex steel 25Cr–7Ni–Mo–N that was modified by the addition of 3 wt% B and processed by spray forming. When compared with the boron-modified supermartensitic steel previously introduced in literature, a higher boron content was added. This boron content was chosen to achieve high abrasive wear resistance. Thermodynamic simulations were used to predict the equilibrium solidification path of the alloy and the equilibrium phases, which were used to explain the experimental results. The boron-modified superduplex steel was additionally subject to abrasive wear testing and the results were correlated to the microstructure observed.

II. EXPERIMENTAL PROCEDURE

The starting material was a commercial superduplex steel grade 6A, according to the standard A890/A890M-13.[23] Table I presents the typical chemical composition of this superduplex steel grade. To adjust the composition, Fe–B, pure Fe and Cr with purity >99.5% were used. Firstly, the raw materials were induction melted in a crucible lined with a silica-alumina refractory. Afterward, the molten metal was spray formed using a close-coupled atomiser under a nitrogen atmosphere. The pouring temperature was approximately 1700 °C and the atomization gas pressure was 0.4 MPa. The spray-formed deposit was applied onto a rotating mild steel substrate resulting in discs of approximately 3.6 kg with 250 mm in diameter and 21 mm in thickness.

Different chemical analysis techniques were carried out to determine the chemical composition of the spray-formed deposit. The carbon content was measured by high-temperature combustion followed by infrared detection (LECO System, St. Joseph, Michigan). The remaining elements were assessed by ICP-AES (Inductive-Coupled Plasma Atomic Emission Spectroscopy) with the exception of boron. The boron content was analyzed by atomic absorption spectroscopy. Based on experimental try-outs, the boron content of 3.0 wt% was selected to induce the formation of a significant quantity of hard borides, in the range of 30–40% in volume.

To predict the solidification path and to understand the microstructural formation of the spray-formed boron-modified superduplex with 3%B (hereinafter named SD-3%B), thermodynamic simulations using the software Thermo-Calc[24] (TCFE7 database, Stockholm, 2012) were carried out. The amount of phases was calculated considering equilibrium conditions.

Structural characterization was conducted by x-ray diffraction using a Siemens D5000 diffractometer (Bruker Corporation, Karlsruhe, Germany) with Cu K_α radiation.

TABLE I. Chemical composition of the superduplex stainless steel grade 6A according to the ASTM A890/A890M-13.

%Fe	%Cr	%Ni	%Mo	%Mn	%Si	%N	%C
Balance	24–26	6.5–8.5	3.0–4.0	1.00 max	1.00 max	0.10–0.30	0.03 max

The 2θ scanning was recorded from 20 to 90°. The microstructural investigation was carried out by Optical and Scanning Electron Microscopy. An optical microscope Olympus BX41M-LED (Olympus, Tokyo, Japan) and a scanning electron microscope (SEM) FEG-XL30 from Phillips (FEI Company, Hillsboro, Oregon) with Oxford EDX analysis system were used. Electron Backscatter Diffraction patterns (EBSD) were recorded using a FEI Quanta 200 (FEI Company) with an EDAX/TSL system.

Hardness measurements were carried out using a Wolpert Testor durometer (Wolpert Wilson Instruments, Aachen, Germany) on the Rockwell C scale. A total of 5 measurement points were carried out with a conical diamond indenter and preload of 10 kgf followed by a load of 150 kgf. The wear resistance was evaluated by dry sand/rubber wheel test, according to procedure A of the ASTM G-65 Standard.[25] Specimens were cut from the deposits by electrical discharge machining in the dimensions of 76 × 25 × 10 mm. Dry sand/rubber wheel test was conducted with a load of 130 N and 200 rpm wheel speed during a total time of 30 min. As abrasive material, sand AFS 50/70 mesh (297–210 μm) was applied with a feed rate of 350 g/min.

III. RESULTS

Table II presents the chemical composition measured in the spray-formed boron-modified superduplex steel.

TABLE II. Chemical composition of spray formed SD-3.0%B.

%Fe	%Cr	%Ni	%Mo	%Mn	%Si	%B	%N	%C
Balance	24.95	5.51	2.48	1.05	1.01	3.00	0.1	0.06

The addition of 3.0 wt% B led to a small change in the overall chemical composition of the base material, reducing slightly the contents of Cr, Ni, Mo, and N and increasing slightly the C content. In terms of Cr, Ni, Mo, and N (not considering the boron content) the final chemical composition matches the superduplex Grade 6A according to the A890/890M-13.

Figure 1 shows the results of the thermodynamic simulations conducted using the chemical composition displayed in Table II. Figure 1(a) shows an isopleth phase diagram with boron content ranging from 0.0 to 4.0 wt%. One can see that the SD-3%B is an hypereutectic composition with the primary phase being the M_2B-type boride. The M_2B boride phase (M = Fe, Cr, Mo, Ni) is very hard and brittle with Vickers hardness >1500,[26] which should lead to an increase in the wear resistance of the boron-modified steel. The presented phase diagram indicates that the equilibrium solidification path of this alloys is quite complex with several reactions taking place during solidification, especially in the range of 1350–1250 °C. Upon cooling, the solidification starts with the formation of the primary M_2B phase until 1340 °C, when the δ-ferrite is formed through the eutectic reaction $L \rightarrow M_2B + \delta$. At lower temperatures the γ-austenite starts to form in a field where four phases coexist: liquid, M_2-B, δ-ferrite, and γ-austenite. Subsequently, the M_3B_2-type boride, which is usually known for being a Mo-rich phase, starts to form in a field with the five phases coexisting. The solidification finishes with a reaction that involves the consumption of the δ-ferrite and the formation of M_3B_2 from the last available liquid.

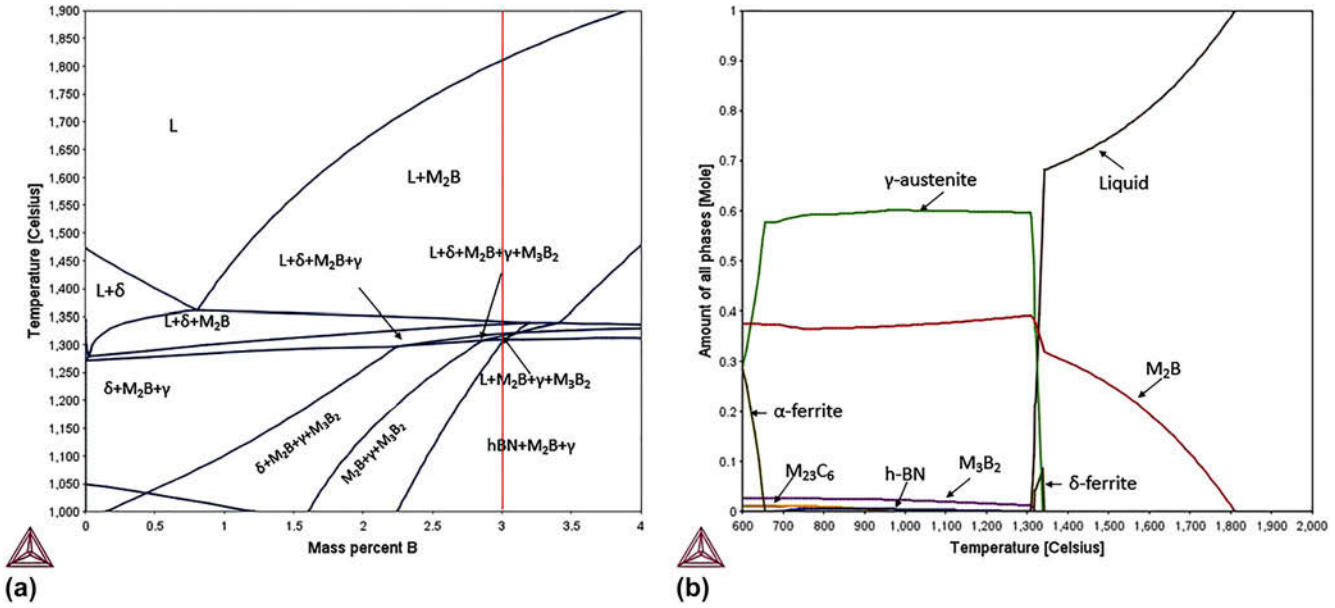

FIG. 1. Thermodynamic calculations: (a) isopleth phase diagram of the SD-3.0%B as a function of B content, (b) stability of phases according to the temperature of the SD-3.0%B.

When the equilibrium solidification path takes place, the as-solidified SD-3%B microstructure is only composed of M_2B, γ-austenite and M_3B_2. Figure 1(b) shows the phase stability diagram of the SD-3%B with the mole fraction of each phase as a function of temperature. The phase fraction just below the *solidus* temperature is 59.5% of γ-austenite, 39.0% of M_2B, and 1.5% of M_3B_2. Observing both diagrams from Fig. 1, the equilibrium calculations predicted that the M_3B_2 fraction slightly increases in a solid–state reaction while the M_2B fraction decreases. Furthermore, the results showed that the hexagonal boron nitride (h-BN) is stable at lower temperatures and may form a solid–state reaction. Nevertheless, both events are very unlikely to occur since boron has an extremely low solubility in the steel phases, which considerably limits the reaction of boron in the solid state. In Fig. 1(b) it can be seen that at around 950 °C the $M_{23}C_6$-type carbides starts to precipitate. Besides, at about 655 °C the α-ferrite begins to precipitate and at 600 °C the fraction of γ-austenite and α-ferrite is balanced (28% each), which would result in the duplex microstructure of the matrix.

Figure 2 shows the diffractogram of the spray-formed SD-3%B. The peaks show the presence of α-ferrite, γ-austenite, and M_2B-type borides. Figure 3 presents SEM (BSE) images of the SD-3%B microstructure. A small quantity of residual porosity appeared as dark spots, which is typical of the spray forming process. In Fig. 3(a) it is possible to identify large borides as the pronounced rod/bulky particles which are the primary M_2B. A eutectic-like phase next to the primary M_2B can be seen with detail in Fig. 3(b).

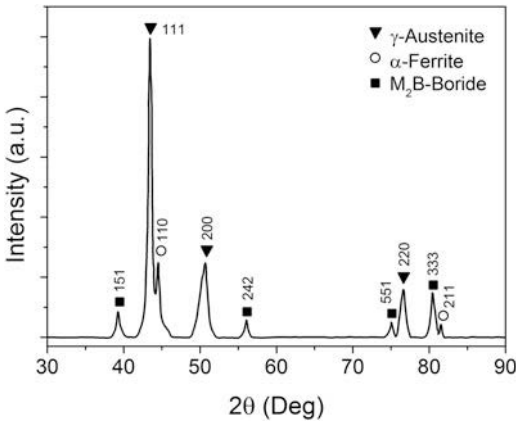

FIG. 2. X-ray diffraction pattern of the spray formed SD-3.0%B.

As described in the equilibrium solidification path previously presented, both the M_2B and the M_3B_2 are formed in sequence through a eutectic reaction. The brighter contrast in the BSE image of the eutectic phase suggests the presence of a heavy element, indicating that the Mo-rich M_3B_2 is in fact present. This result corroborates with the EDX dot-mapping displayed in Fig. 4, which clearly shows that the regions next to the primary M_2B-type borides are indeed richer in Mo. These borides are embedded in an austenitic/ferritic matrix. By observing the BSE image of Fig. 3(b) and the EBSD image in Fig. 5, one can see that the ferrite is always present next to the primary M_2B borides. As demonstrated by thermodynamic simulations, the as-solidified microstructure of the SD-3%B is ferrite-free. Moreover, it was shown that this phase precipitates at lower temperatures. Thus, the borides interface may act as a nucleation site, which favors the formation of the α-ferrite next to the M_2B. Probably, due to the small content of carbon and nitrogen, fractions of minor phases such as carbides or nitrogen-containing phases, if present, could not be identified by the characterization techniques carried out in this work.

The contents and distribution of the main microstructural constituents, namely α-ferrite, γ-austenite, and M_2B-type borides were investigated by EBSD. As shown in Fig. 5, a good index quality map was obtained for the identification of phases (left). However, it is worth stressing that only the primary M_2B could be indexed while the eutectic constituent containing the M_3B_2, probably due to its small size, could not be indexed. The ferrite and austenite grains were quite small with less than 10 μm in size and also randomly distributed. Estimated phase fractions were around 31% for α-ferrite, 34% for

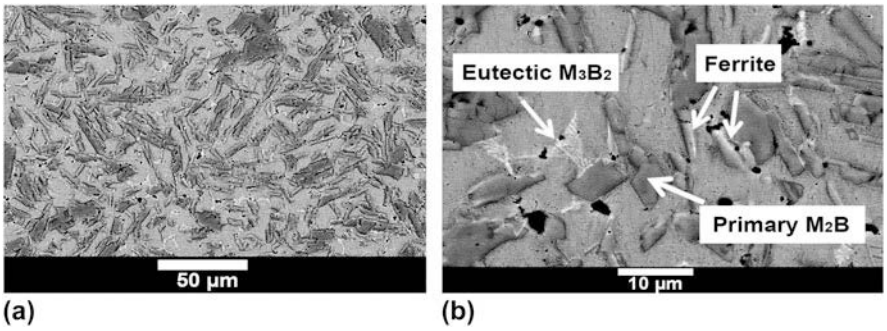

FIG. 3. Scanning electron micrographs-SEM of the spray formed SD-3.0%B recorded with the backscatter electron detector: (a) overview showing the main microstructural constituents and (b) detail of borides.

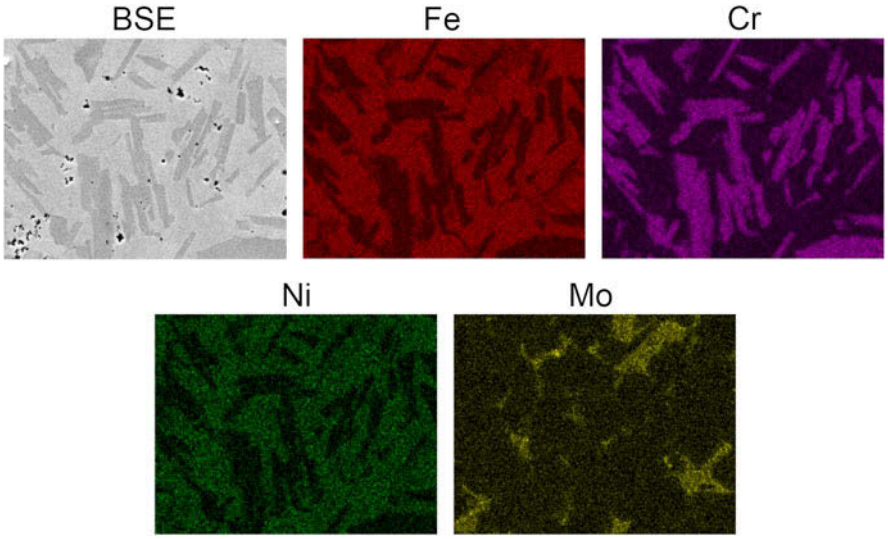

FIG. 4. EDX dot-mapping of spray formed the SD-3.0%B.

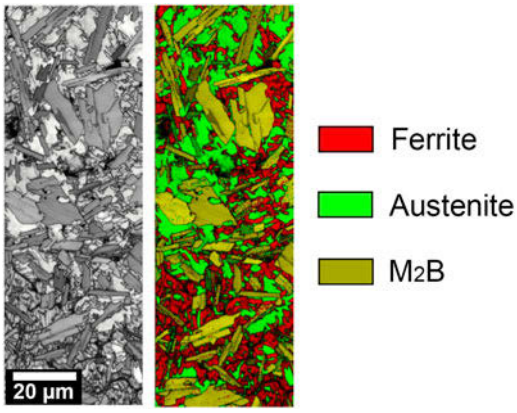

FIG. 5. EBSD measurement for phase identification of the SD-3.0%B.

γ-austenite, and 35% for M_2B-type boride. This result is in good agreement with the predicted phase fraction shown in Fig. 1(b) at 600 °C.

The Rockwell C hardness and wear performance measured with the dry sand/rubber wheel test are shown in Fig. 6. The combined effects of spray forming process and boron modification are quite remarkable resulting in an increase from 23 to 47 HRC in hardness. The cobalt-based alloy Stellite 1016 was the hardest material with almost 12 HRC difference to the spray-formed SD-3%B. Nonetheless, the worn volumes of both materials were at the same level. The largest difference in wear resistance is found comparing the as-cast SD steel grade 6A with the spray-formed SD-3%B that reached a factor of about 3.6 times.

IV. DISCUSSION

This work presents a first attempt to produce a wear-resistant spray-formed boron-modified superduplex stainless steel with considerably high boron content (3 wt%). Furthermore, thermodynamic simulations of the stable phases under equilibrium conditions were conducted aiming at predicting the final microstructure of the spray-formed alloy to better understand the microstructure formation. The calculation of phase's stability and equilibrium solidification path were based on a previous work[22] from which the authors have shown that the solidification of spray-formed steels takes place under near equilibrium conditions. By analysing the microstructure of the overspray powders and the spray-formed deposits of two different steel grades, a high alloyed tool steel (AISI D2) and a boron-modified supermartensitic stainless steel with 0.3 wt% and 0.7 wt%, the authors proposed a solidification model for spray-formed steels.[22]

The solidification model states that when the set of fully liquid, partially liquid, and fully solidified droplets impinge the deposition zone, the droplets are thermally balanced until a temperature above the alloy's *solidus* temperature (for satisfactory processing conditions). Due to the small size of the deposited droplets (few hundred of microns) and the high thermal diffusivity of steels, this thermal balance occurs considerably fast (less than 0.1 s).[15] Once the equilibrium temperature lies in the liquid/solid field the completely solidified droplets are partially remelted and/or dissolved in such a way that the phases fraction is changed till reaching the equilibrium phase fraction (or approximately the equilibrium fraction) at that equilibrium temperature. The continuous heat input delivered to the deposition zone by the continuous impingement of the atomised droplets favors this phase fraction balance. Moreover, the continuous droplets impingement also favors the thermal and chemical homogenization of the liquid present in the deposition zone, which becomes continuous throughout the

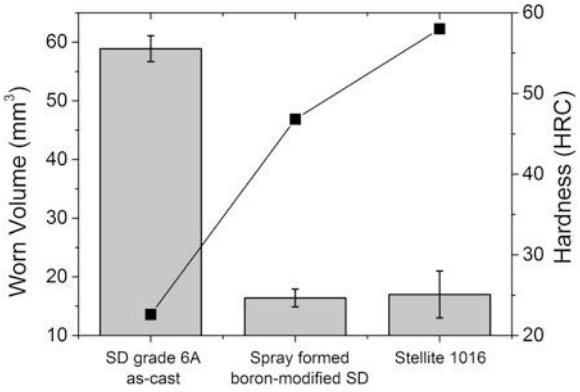

FIG. 6. Rockwell C hardness values (right *Y*-axis) and wear test results (left *Y*-axis) as a function of different alloys. Values of Stellite 1016 were taken from the standard ASTM G-65.[25]

deposition zone when the phase fraction equilibration occurs. The developing of equiaxed grains characteristic of most of the spray-formed alloys is attributed to the high homogeneous thermal gradient (caused by the turbulence promoted by the continuous droplets impingement) around the primary nuclei that favors them to grow without any preferential direction.

The thermodynamic simulations carried out in this work showed that the equilibrium solidification path of the SD-3%B is quite complex involving several reactions and phases (M_2B, γ-austenite, δ-ferrite and M_3B_2). In contrast to the boron-modified supermartensitic stainless steel previously reported,[13] with the solidification path comprising only the formation of primary γ-austenite followed by the eutectic reaction $L \rightarrow \gamma + M_2B$. Although the higher complexity of the SD-3%B solidification path, the phases present in the final spray-formed deposit were accurately predicted by the thermodynamic calculations. This result demonstrated that the thermodynamic simulation can indeed be a powerful tool for designing spray-formed alloys. In addition to that, new insights could be taken regarding the solidification of spray-formed steels. One can see that the final microstructure of the spray-formed SD-3%B does not have an equiaxed microstructure that is usually reported as characteristic of spray-formed alloys. The reason for this is that the primary phase formed is the intermetallic M_2B-type boride, which grows into the liquid as a faceted phase. When this sort of faceted intermetallic phase is formed, the thermal homogenization of the liquid within the deposition zone is not enough to allow its equiaxial growth (as in the case of the primary γ-austenite). Consequently, spray-formed alloys with faceted primary phases are unlikely to present equiaxed grains.

The solidification sequence of the SD-3%B described by the thermodynamic simulations seems to fit the final spray-formed deposit, which can be seen by the formation of the primary M_2B and the formation of the eutectic constituent composed of the Mo-rich M_3B_2. Nevertheless, it must be stressed that, after solidification, the amount of equilibrium phases considerably changes under cooling in the solid state. The thermodynamic simulation predicted that the fraction of M_2B and the M_3B_2 change, as well as the precipitation of the hexagonal boron nitride under cooling. However, because of the extremely low solubility of boron in the iron phases (<0.0008 wt%[27]), the reactions involving the borides in solid state is unlikely to occur. On the other hand, if the cooling rate of the spray-formed deposit is sufficiently low, the phase transformation from γ-austenite to α-ferrite should take place. According to calculated values as well as experimental data, the cooling rate of deposits of spray-formed steel is typically in the order of 0.3 °C/s.[22,28] This cooling rate is low enough to allow the γ to α phase transition to occur. The EBSD measurements demonstrated that the fraction of both phases (31% for α-ferrite and 34% for γ-austenite) are approximately those predicted at 600 °C (28% for α-ferrite and 27% for γ-austenite), which is a reasonable threshold temperature for the occurrence of this phase transformation. At temperatures below 600 °C the phase transition kinetics are likely to be slow because of the low diffusivity. These results are quite interesting once they show that the spray-formed microstructure of the boron-modified stainless steel grades can be reasonably predicted by thermodynamic simulations under equilibrium conditions.

Due to the formation of hard borides and the fine microstructure originated from spray forming, the hardness and wear resistances could be significantly improved, as shown in Fig. 6. According to many research works,[13,14,29–32] borides are quite effective at improving hardness and the wear behavior of steels. In case of the dry sand/rubber wheel test, the hardness of the matrix is important, but also if hard particles (borides) are present, their phase fractions and sizes.[33] Consequently, the presence of significant amount of borides (>30%) homogeneously distributed in the microstructure was responsible for the efficient shielding of the superduplex matrix from material removal. The result presented in this paper for the spray-formed SD-3%B was even comparable to a hardfacing material (Stellite 1016) that contains carbides as reinforcing particles. This result shows that the strategy of designing boron-modified stainless steel aiming at increasing the wear resistance while maintaining the stainless steel matrix features is feasible and quite attractive based on the abrasive wear resistance of the SD-3%B, which is in the same level of the extensively used Co-based alloys that are considerably more expensive.

V. CONCLUSIONS

The following conclusions could be drawn from this investigation:

(1) Spray forming of boron-modified superduplex stainless steel with 3 wt% B led to the formation of a

fine-grained microstructure containing α-ferrite, γ-austenite, and borides with different morphologies: primary M_2B and eutectic M_2-B/M_3B_2.

(2) Due to the formation of a primary M_2B boride, the final microstructure was not equiaxial, as normally found in spray-formed alloys.

(3) A good agreement of thermodynamic simulations under equilibrium conditions and the final spray-formed microstructures of the superduplex stainless steel with 3 wt% B was observed.

(4) The spray formed superduplex stainless steel showed comparable wear resistance to the hardfacing material Stellite 1016 in the dry sand/rubber wheel test. The high phase fraction of borides was responsible for the outstanding wear resistance.

ACKNOWLEDGMENTS

The authors would like to thank the Brazilian research funding agencies FAPESP (grant No. 2014/27073-0), CNPq and CAPES for the financial support and the company PETROBRAS for sponsoring this research.

REFERENCES

1. L. Gardner: The use of stainless steel in structures. *Prog. Struct. Eng. Mater.* **7**(2), 45–55 (2005).
2. N.R. Baddoo: Stainless steel in construction: A review of research, applications, challenges and opportunities. *J. Constr. Steel Res.* **64**(11), 1199–1206 (2008).
3. J-O. Nilsson: Super duplex stainless steels. *Mater. Sci. Technol.* **8**(8), 685–700 (1992).
4. R.N. Gunn: *Duplex Stainless Steels: Microstructure, Properties and Applications*, 1st ed. (Woodhead Publishing, Cambridge, 1997).
5. I. Alvarez-Armas and S. Degallaix-Moreuil: *Duplex Stainless Steels*, 1st ed. (John Wiley & Sons, Hoboken, 2013).
6. ASM International: *ASM Handbook Volume 18: Friction, Lubrication, and Wear Technology* (ASM International, Materials Park, 1992).
7. P.J.E. Monson and W.M. Steen: Comparison of laser hardfacing with conventional processes. *Surf. Eng.* **6**(3), 185–193 (1990).
8. B.G. Mellor: *Surface Coatings for Protection Against Wear*, 1st ed. (Woodhead Publishing, Cambridge, 2006).
9. D-G. Ahn: Hardfacing technologies for improvement of wear characteristics of hot working tools: A review. *Int. J. Precis. Eng. Manuf.* **14**(7), 1271–1283 (2013).
10. F.A.P. Fernandes, S.C. Heck, R.G. Pereira, C.A. Picon, P.A.P. Nascente, and L.C. Casteletti: Ion nitriding of a superaustenitic stainless steel: Wear and corrosion characterization. *Surf. Coat. Technol.* **204**(18–19), 3087–3090 (2010).
11. A. Gholipour, M. Shamanian, and F. Ashrafizadeh: Microstructure and wear behavior of stellite 6 cladding on 17-4 PH stainless steel. *J. Alloys Compd.* **509**(14), 4905–4909 (2011).
12. L. Ceschini, C. Chiavari, E. Lanzoni, and C. Martini: Low-temperature carburised AISI 316L austenitic stainless steel: Wear and corrosion behaviour. *Mater. Des.* **38**, 154–160 (2012).
13. G. Zepon, A.R.C. Nascimento, A.H. Kasama, R.P. Nogueira, C.S. Kiminami, W.J. Botta, and C. Bolfarini: Design of wear resistant boron-modified supermartensitic stainless steel by spray forming process. *Mater. Des.* **83**, 214–223 (2015).
14. E. Sigolo, J. Soyama, G. Zepon, C.S. Kiminami, W.J. Botta, and C. Bolfarini: Wear resistant coatings of boron-modified stainless steels deposited by plasma transferred arc. *Surf. Coat. Technol.* **302**, 255–264 (2016).
15. P.S. Grant: Solidification in spray forming. *Metall. Mater. Trans. A* **38**(7), 1520–1529 (2007).
16. T. Ebert, F. Moll, and K.U. Kainer: Spray forming of magnesium alloys and composites. *Powder Metall.* **40**(2), 126–130 (1997).
17. P.S. Grant: Spray forming. *Prog. Mater. Sci.* **39**(4–5), 497–545 (1995).
18. C. Banjongprasert, S.C. Hogg, E. Liotti, C.A. Kirk, S.P. Thompson, J. Mi, and P.S. Grant: Spray forming of bulk ultrafine-grained Al–Fe–Cr–Ti. *Metall. Mater. Trans. A* **41**(12), 3208–3215 (2010).
19. L. Lu, L. Hou, J. Zhang, H. Wang, H. Cui, J. Huang, Y. Zhang, and J-S. Zhang: Microstructure characteristics of spray-formed high speed steel and its evolution during subsequent hot deformation. *J. Mater. Res.* **31**(2), 274–280 (2016).
20. R. Su, Y. Qu, J. You, and R. Li: Study on a new retrogression and re-aging treatment of spray formed Al–Zn–Mg–Cu alloy. *J. Mater. Res.* **31**(5), 573–579 (2016).
21. A. Schulz, V. Uhlenwinkel, C. Escher, R. Kohlmann, A. Kulmburg, M.C. Montero, R. Rabitsch, W. Schützenhöfer, D. Stocchi, and D. Viale: Opportunities and challenges of spray forming high-alloyed steels. *Mater. Sci. Eng., A* **477**(1–2), 69–79 (2008).
22. G. Zepon, N. Ellendt, V. Uhlenwinkel, and C. Bolfarini: Solidification sequence of spray-formed steels. *Metall. Mater. Trans. A* **47**(2), 842–851 (2015).
23. ASTM International: *ASTM A890/A890M-13—Standard Specification for Castings, Iron–Chromium–Nickel–Molybdenum Corrosion-Resistant, Duplex Austenitic/Ferritic for General Application* (ASTM International, West Conshohocken, 2013).
24. B. Sundman, B. Jansson, and J-O. Andersson: The Thermo-Calc databank system. *Calphad* **9**(2), 153–190 (1985).
25. ASTM International: *ASTM G65-G15 Standard Test Method for Measuring Abrasion Using the Dry Sand/Rubber Wheel Apparatus* (ASTM International, West Conshohocken, 2015).
26. V.I. Matkovich: *Boron and Refractory Borides*, 1st ed. (Springer-Verlag, Berlin, 1977).
27. A.A. Azarkevich, L.V. Kovalenko, and V.M. Krasnopolskii: The optimum content of boron in steel. *Met. Sci. Heat Treat.* **37**(1), 22–24 (1995).
28. C. Cui, U. Fritsching, A. Schulz, R. Tinscher, K. Bauckhage, and P. Mayr: Spray forming of homogeneous 100Cr6 bearing steel billets. *J. Mater. Process. Technol.* **168**(3), 496–504 (2005).
29. L. Bourithis and G. Papadimitriou: Boriding a plain carbon steel with the plasma transferred arc process using boron and chromium diboride powders: Microstructure and wear properties. *Mater. Lett.* **57**(12), 1835–1839 (2003).
30. M. Darabara, G.D. Papadimitriou, and L. Bourithis: Tribological evaluation of Fe–B–TiB_2 metal matrix composites. *Surf. Coat. Technol.* **202**(2), 246–253 (2007).
31. L. Bourithis and G.D. Papadimitriou: The effect of microstructure and wear conditions on the wear resistance of steel metal matrix composites fabricated with PTA alloying technique. *Wear* **266**(11–12), 1155–1164 (2009).
32. D. Liu, R. Liu, Y. Wei, Y. Ma, and K. Zhu: Microstructure and wear properties of Fe–15Cr–2.5Ti–2C–xB wt% hardfacing alloys. *Appl. Surf. Sci.* **271**, 253–259 (2013).
33. L. Bourithis and G. Papadimitriou: Three body abrasion wear of low carbon steel modified surfaces. *Wear* **258**(11–12), 1775–1786 (2005).